2022

# Reducing Print Time While Minimizing Loss in Mechanical Properties in Consumer FDM Parts

Long Le
*Old Dominion University*

Mitchel A. Rabsatt
*Old Dominion University*

Hamid Eisazadeh
*Old Dominion University*

Mona Torabizadeh
*Old Dominion University*



## Original Publication Citation

Le, L., Rabsatt, M. A., Eisazadeh, H., & Torabizadeh, M. (2022). Reducing print time while minimizing loss in mechanical properties in consumer FDM parts. *International Journal of Lightweight Materials and Manufacture, 5*(2), 197-212. https://doi.org/10.1016/j.ijlmm.2022.01.003

International Journal of Lightweight Materials and Manufacture 5 (2022) 197–212

Contents lists available at ScienceDirect

International Journal of Lightweight Materials and Manufacture

journal homepage: https://www.sciencedirect.com/journal/international-journal-of-lightweight-materials-and-manufacture

Original Article

# Reducing print time while minimizing loss in mechanical properties in consumer FDM parts

Long Le [a], Mitchel A. Rabsatt [a], Hamid Eisazadeh [b, *], Mona Torabizadeh [b]

[a] Mechanical and Aerospace Engineering Department, Old Dominion University, Norfolk, VA 23518, USA
[b] Engineering Technology Department, Old Dominion University, Norfolk, VA 23518, USA

ARTICLE INFO

*Article history:*
Received 19 December 2021
Accepted 25 January 2022
Available online 1 February 2022

*Keywords:*
3D printing
Fused deposition modeling (FDM)
Tensile strength
Thermoplastics
Polylactic acid (PLA)
Design of experiments (DOE)

ABSTRACT

Fused deposition modeling (FDM), one of various additive manufacturing (AM) technologies, offers a useful and accessible tool for prototyping and manufacturing small volume functional parts. Polylactic acid (PLA) is among the commonly used materials for this process. This study explores the mechanical properties and print time of additively manufactured PLA with consideration to various process parameters. The objective of this study is to optimize the process parameters for the fastest print time possible while minimizing the loss in ultimate strength. Design of experiments (DOE) was employed using a split-plot design with five factors. Analysis of variance (ANOVA) was employed to verify the model significance or otherwise. Once the model was developed, confirmation points were run to validate the model. The model was confirmed since the observations at the optimum were within the prediction interval with a confidence value of 95%. Then, the model was used to assess the ultimate strength and print time of FDM parts with consideration to nozzle diameter, the number of outer shells, extrusion temperature, infill percentage, and infill pattern. Recommendations are discussed in detail in this study to reduce print time without sacrificing significant part strength.


## 1. Introduction

Fused deposition modeling (FDM), one of various additive manufacturing (AM) technologies, has revolutionized the manufacturing industry, from the development of concept models to the creation of functional parts. FDM uses a wide variety of materials to create 3D printed parts. Material selection is not the only design choice in the FDM process [1]. Process parameters, such as orientations of the build, thermal conditions, and slicing parameters are just as important since they affect the ultimate strength of the 3D printed parts. Common building orientations, e.g. how the part is positioned when produced [2], are horizontal, vertical, and lateral, but other desired orientations, such as inclined, may be used as well. Thermal conditions like bed, extrusion, and ambient temperatures play an important role in the shrinkage of the parts and adhesion with the previously deposited layers. The effect of these process parameters on the mechanical properties were investigated in the literature [3,4]. It has been shown that mechanical anisotropy in FDM 3D printed parts is an inherent nature of all AM methods, which is almost unavoidable due to the presence of voids in the final printed parts' structure [5–8]. Throughout many studies on the topic of FDM, the literature shows that significant limitation of the FDM process can be attributed to the anisotropic nature of the parts that it produces [9]. Often the adhesion between the layers is what defines the strength of an FDM part rather than the material itself [10].

Infill percentage and pattern are two other process parameters affecting the mechanical properties of 3D printed parts [11,12]. One recent study sought to fill the existing knowledge gap as it relates to the infill percentage of AM parts [11]. In this study, the materials that were tested included PLA, ABS, PETG various nylon, polycarbonates, and ASA filaments at infill percentages ranging from 15% to 100%. The finding of this study revealed that in some materials the infill percentage affected the failure mode of the tested specimens. For example, the authors observed that in the PETG and Nylon 910 specimens at 100% infill the specimens failed in a ductile manner. Whereas at 30%, they failed in a more brittle manner. The

* Corresponding author. Fax: +1 757 683.5655.
*E-mail address:* heisazad@odu.edu (H. Eisazadeh).
Peer review under responsibility of Editorial Board of International Journal of Lightweight Materials and Manufacture.

https://doi.org/10.1016/j.ijlmm.2022.01.003

authors concluded that for all the specimens tested, as the infill percentage decreased, the tensile strength was significantly impacted. In addition, the infill percentage also affected the specimen's modulus and elongation, in addition to the failure modes.

Infill percentage is an important aspect of an additively manufactured part, but there are other factors, such as the number of outer shells used, the type of infill pattern used, the extrusion temperature, and the effects, if any, that the size of the nozzle diameter may have on the part [13]. For instance, Sagias et al. opted to use a design of experiment approach to minimize the variability in the parts' performance in response to noise factors, while maximizing the variability in response to signal factors [14]. The authors achieved this by implementing the Taguchi methodology, which uses specific arrays called orthogonal arrays (OA) that are based on selected arrays in accordance with their respective levels. The authors ranked the factors that had the greatest influence on the parts' mechanical properties. The layer thickness was deemed to have the greatest influence on the parts test, whereas part placement (i.e., orientation) was deemed to have the least influence on the parts tested. Another study, conducted by Vălean et al., investigated the influence of spatial printing directions 0, 45, and 90, and the size effect on specimen mechanical properties [15]. The experiments were carried out using dog bone specimens made of PLA material, adhered to ISO 527-1 standard [15]. The findings of this study revealed that the spatial orientation was highly influential in regard to the tensile strength and was less influential on the Young's modulus.

It is noticed that a good number of works in FDM are devoted to studying the effect of processing conditions on the part strength. In general, most of the mentioned studies showed that complex designs require more time, moves, and amount of material, which all increase the overall fabrication cost. However, no significant effort has been made to develop an understanding of the effects of the nozzle diameter, extrusion temperature, infill percentage, infill pattern, and the number of outer shells in minimizing print time without sacrificing significant part strength. This is particularly critical for lightweight structures of additively manufactured parts where process efficiency should be improved through reducing print time or material use.

This study aims to build upon the existing knowledge and knowledge garnered from various literature reviews to provide a holistic view as to what aspects of the FDM process have the greatest impact on a part's mechanical performance. As such, the objective of this paper is to assess the ultimate strength and print time of additively manufactured PLA with consideration to the aforementioned factors. Stat Ease's Design Expert software is leveraged to conduct the experiment using a split-plot design with five factors. This design was chosen because one of the factors (nozzle diameter) was considered as a hard-to-change (HTC) factor. Parameters like nozzle diameter, the number of outer shells, extrusion temperature, infill pattern, and percentage are calibrated with respect to the print time and the maximum tensile stress for each respective part. Recommendations to reduce print time without sacrificing significant part strength are discussed in detail in this study.

## 2. Experiment

A consumer-grade PLA filament was extruded from a Prusa FFF machine [16] for the production of the dogbone specimens, according to ASTM D638-14 type IV for static tensile testing [17]. Table 1 shows the material information provided by the manufacturer. CAD files of the specimen's geometry were created using Autodesk Fusion 360 and then exported as an STL file. The geometry of the test samples was chosen from the ASTM D618 standard. Fig. 1 illustrates the dimensions of the tensile specimen. All specimens are printed in a horizontal direction, as seen in Fig. 2, to reduce the effects of the anisotropic nature of PLA specimens. This orientation was chosen to replicate how a user would orient a load-bearing part on the build plate, rather than testing for part strength via layer adhesion. A total of 16 samples were printed for quasi-static tensile tests. The Prusa mini printer was employed to manufacture the parts using two extrusion nozzle diameters, 0.4 mm and 0.6 mm.

Prusa's slicing software PrusaSlicer-2.3.0 [18] was used to pre-process the CAD models generating the necessary G-code and tool paths for 3D printing. Since the mechanical performance of the filaments is affected by moisture, all the samples were printed after placing the filament in a filament dryer at 55 °C for 24 h. Once the samples were printed, post-processing was performed on them to remove all brim and extra surface defects that may have an impact on the test results. The samples were then stored in a humidity and temperature-controlled environment at 30% humidity and 72 °F.

To perform the tensile tests, a Zwick Roell zwickiLine z2.5 materials testing machine was used. An extensometer and a transverse strain extensometer were used, in addition to the loading cell that was provided by Zwick Roell to measure elongation. Zwick Roell's testXpert3 data acquisition software was used to record loading data in real-time for each specimen. The specimens were fitted into the tensile jaws, checked for alignment, and then pretensioned to eliminate compressive forces and improve repeatability of the results. The test speed was set to 5 mm/min.

### 2.1. Design of experiment

The experiment was conducted with five factors of interest including nozzle diameter, the number of outer shells, extrusion temperature, infill percentage, and pattern. There are other process parameters that may affect the print time and part strength such as layer height, printing speeds, cooling, etc. This study focuses on the most commonly changed process parameters by consumers. Therefore, the default settings by the manufacturer for each nozzle diameter were used in this study. Flowrate for each nozzle diameter was calibrated by measuring the filament diameter and the amount of material extruded to ensure the proper amount of material was deposited.

In the DOE study, each factor had two levels and the responses were the print time (minutes) and ultimate tensile strength (MPa). The nozzle diameter was considered as a hard-to-change (HTC) factor because it would be time-consuming to change and would require recalibration of the first layer. Due to the HTC factor, a split-plot design was used to hold the HTC factor at a fixed level called whole-plots (WP) while the remaining easy-to-change (ETC) factors were randomized in groups known as sub-plots (SP).

The nozzle diameter affects the overall level of detail in the XY plane, the layer height (typically 80% of the nozzle diameter), and the thickness of each perimeter wall (shell thickness). The interactions between all these factors also impact print speed. For this

**Table 1**
Inland PLA material specifications.

| Diameter | Material | Color | Print temperature | Plate temperature | Density | Tensile strength | Elongation at break |
|---|---|---|---|---|---|---|---|
| 1.75 mm | PLA | White | 205–225 °C | 60–80 °C | 1.24 g/cm$^3$ | 60 MPa | 29% |

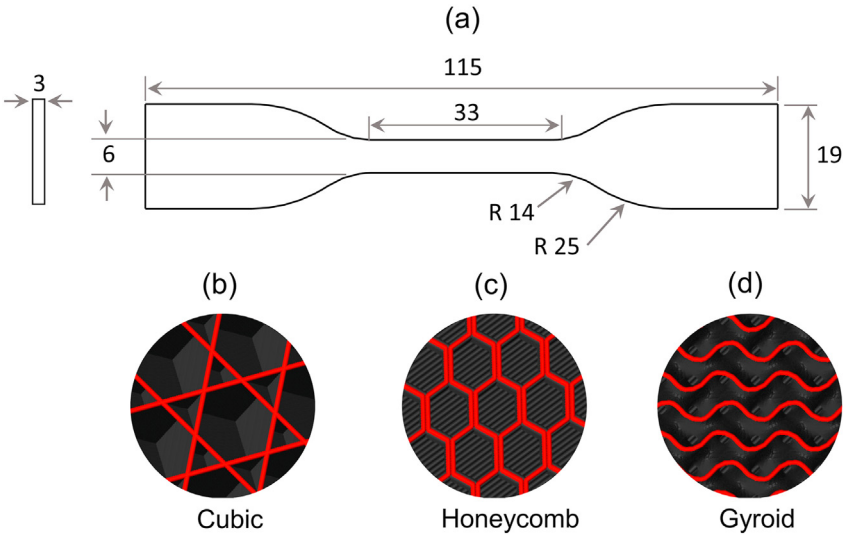


**Fig. 1.** (a) Dimensions of ASTM D638-14 Type IV Dogbone specimen, (b), (c) and (d) three common infill patterns.

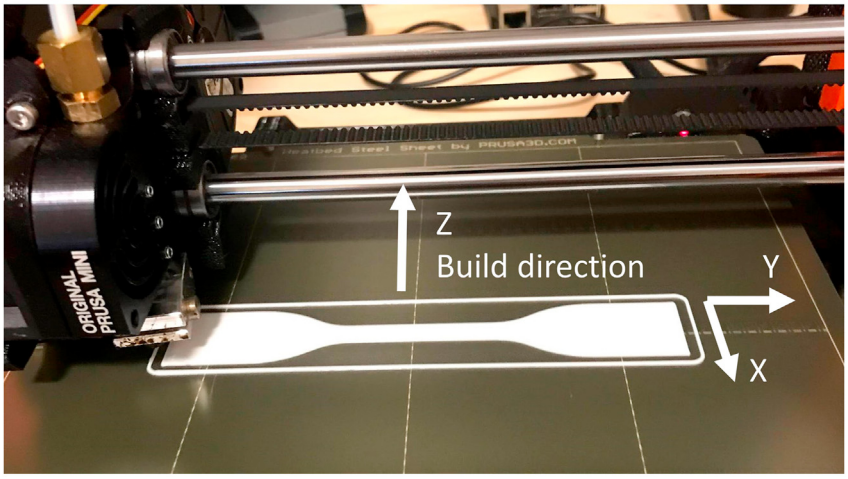


**Fig. 2.** Printed orientation relative to the gravity vector or build direction.

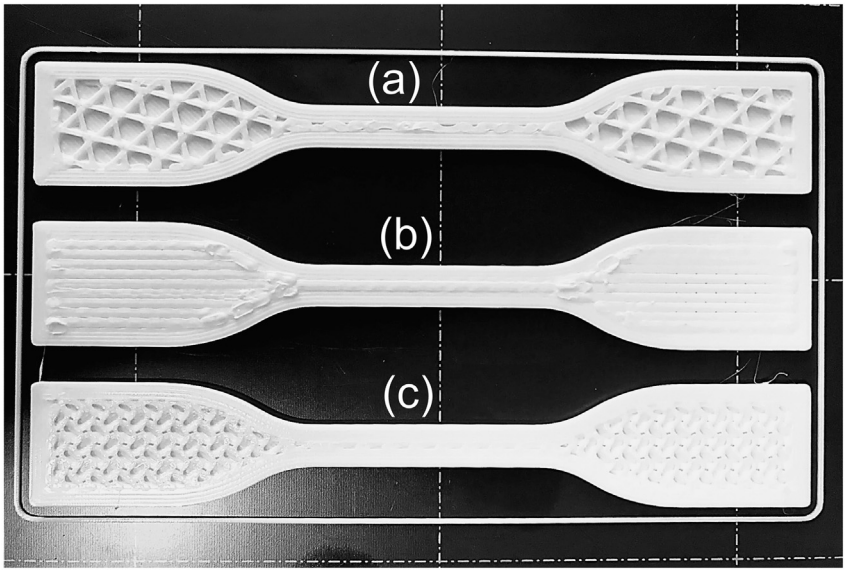


**Fig. 3.** Infill patterns at 40% Infill. (a) cubic, (b) 3D honeycomb, (c) gyroid.

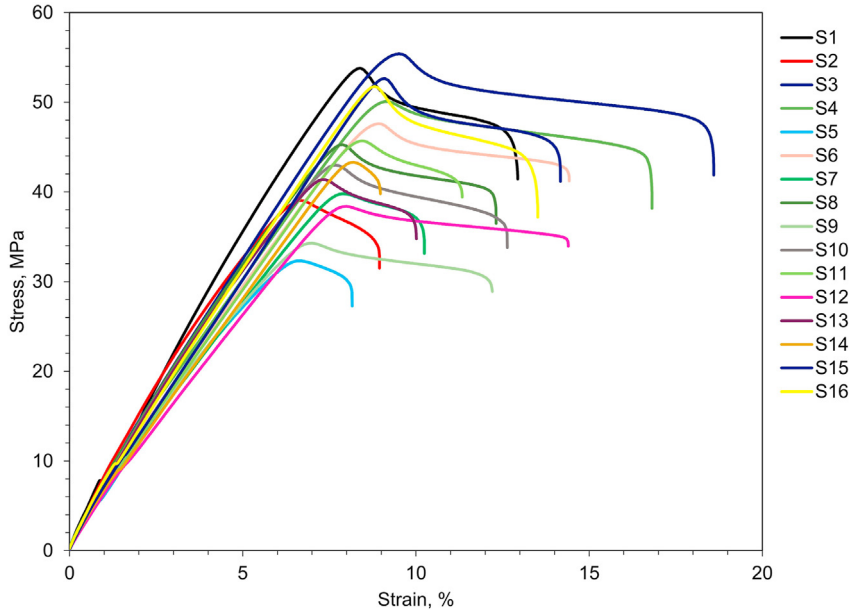


**Fig. 4.** Tensile test results achieved for sixteen samples; process parameters of each run (S1–S16) are represented in Table 2.

**Table 2**
Factors and responses for design of experiment (DOE).

| Group | Run | Factor 1 | Factor 2 | Factor 3 | Factor 4 | Factor 5 | Response 1 | Response 2 |
|---|---|---|---|---|---|---|---|---|
| | | a: Nozzle dia. (mm) | B: Shells | C: Filament temp. (°C) | D: Infill % (%) | E: Infill pattern | Print time (min) | Strength (MPa) |
| 1 | 1 | 0.6 | 4 | 215 | 10 | Cubic | 15 | 53.8 |
| 1 | 2 | 0.6 | 2 | 230 | 10 | Cubic | 13 | 39.1 |
| 1 | 3 | 0.6 | 4 | 215 | 40 | Gyroid | 17 | 55.4 |
| 1 | 4 | 0.6 | 2 | 230 | 40 | Gyroid | 16 | 50.1 |
| 2 | 5 | 0.4 | 2 | 215 | 10 | Cubic | 17 | 32.4 |
| 2 | 6 | 0.4 | 4 | 230 | 40 | Gyroid | 25 | 47.7 |
| 2 | 7 | 0.4 | 2 | 230 | 40 | Cubic | 20 | 39.8 |
| 2 | 8 | 0.4 | 4 | 215 | 10 | Gyroid | 20 | 45.3 |
| 3 | 9 | 0.4 | 2 | 230 | 10 | Gyroid | 18 | 34.3 |
| 3 | 10 | 0.4 | 4 | 230 | 10 | Cubic | 20 | 43 |
| 3 | 11 | 0.4 | 4 | 215 | 40 | Cubic | 23 | 45.7 |
| 3 | 12 | 0.4 | 2 | 215 | 40 | Gyroid | 24 | 38.4 |
| 4 | 13 | 0.6 | 2 | 215 | 10 | Gyroid | 13 | 41.4 |
| 4 | 14 | 0.6 | 2 | 215 | 40 | Cubic | 15 | 43.3 |
| 4 | 15 | 0.6 | 4 | 230 | 40 | Cubic | 17 | 52.7 |
| 4 | 16 | 0.6 | 4 | 230 | 10 | Gyroid | 15 | 51.8 |

experiment, a default layer height of 200 μm was maintained between the two factor levels as it was the common layer height in the preset settings by Prusa between the two selected nozzle diameters. The standard nozzle diameter used by most current 3D printers is 0.4 mm, which is manufactured by E3D [19] on the test machine in this experiment. A 0.6 mm nozzle is the next larger size diameter available by E3D that doesn't sacrifice a significant amount of detail. Therefore, the factor levels selected for the nozzle diameter were 0.4 mm and 0.6 mm. These were considered categorical factors. Further details of nozzle diameter effect on part strength are discussed later in this study.

The number of outer shells is determined by the settings for the number of perimeter walls and the number of top and bottom layers. The standard settings are two perimeter walls, along with two top and two bottom layers. Therefore, the lower level for this factor was set to two walls for the outer shell. The high level was determined by using the 0.6 mm nozzle (increased wall thickness), zero top layers, two bottom layers, and increasing the number of perimeter walls until the reduced section of the test specimen was near solid. It was found that the reduced section would be solid at five perimeter walls, therefore, the high level was set to four walls for the shell.

The extrusion temperature affects the adhesion between each layer, which in turn affects the strength of the part [3]. Additionally, the extrusion temperature can also affect the quality of the print [15]. With higher extrusion temperatures, the thermoplastic will begin to become too soft and flimsy, leading to a difficult print. With lower extrusion temperatures, the poor diffusion and entanglement of chains between filaments may occur during the deposition process [5]. In this study, the low level of this factor was set to the manufacturer's recommendation of 215 °C. The high level was set to 230 °C (15 °C above the manufacturer's recommendation), which was the highest temperature before the calibration prints became difficult. Further details of the nozzle temperature effect on part strength is discussed later in this study.

The infill settings are used for the area within the outer shells. This includes the infill pattern along with the infill percentage. PrusaSlicer-2.3.0 offers different patterns for functional prints,

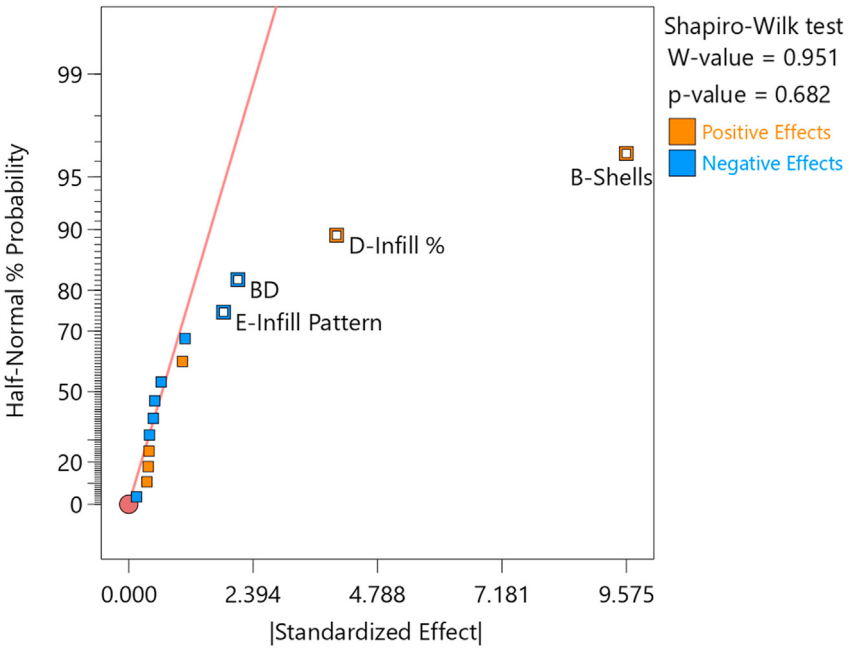


**Fig. 5.** Half-normal probability plot of subplot effects for ultimate strength.

**Table 3**
ANOVA table for maximum ultimate strength, fixed effects [Type III], performed by REML (restricted maximum likelihood) analysis.

| Source | Term df | Error df | F-value | p-value | |
|---|---|---|---|---|---|
| **Whole-plot** | 1 | 2.00 | 37.56 | 0.0256 | Significant |
| a-Nozzle dia. | 1 | 2.00 | 37.56 | 0.0256 | |
| **Subplot** | 4 | 8.00 | 62.45 | <0.0001 | Significant |
| B-Shells | 1 | 8.00 | 198.43 | <0.0001 | |
| D-Infill % | 1 | 8.00 | 34.63 | 0.0004 | |
| E-Infill pattern | 1 | 8.00 | 7.21 | 0.0277 | |
| BD | 1 | 8.00 | 9.54 | 0.0149 | |

meaning they provide support on the outer shells evenly in all directions. These patterns include cubic, 3D honeycomb, and gyroid, as shown in Fig. 1. The infill percentage factor levels were determined by printing each pattern at increasing infill percentages until the reduced section of the test specimen was near solid, similar to determining the number of perimeter walls. This was done using the 0.6 mm nozzle, zero top layers, two bottom layers, and four perimeter walls. It was found that the 3D honeycomb pattern would result in a solid test specimen throughout the entire part with infill percentages above 25% percent. Due to the low infill percentage range, this pattern was discarded from the experiment.

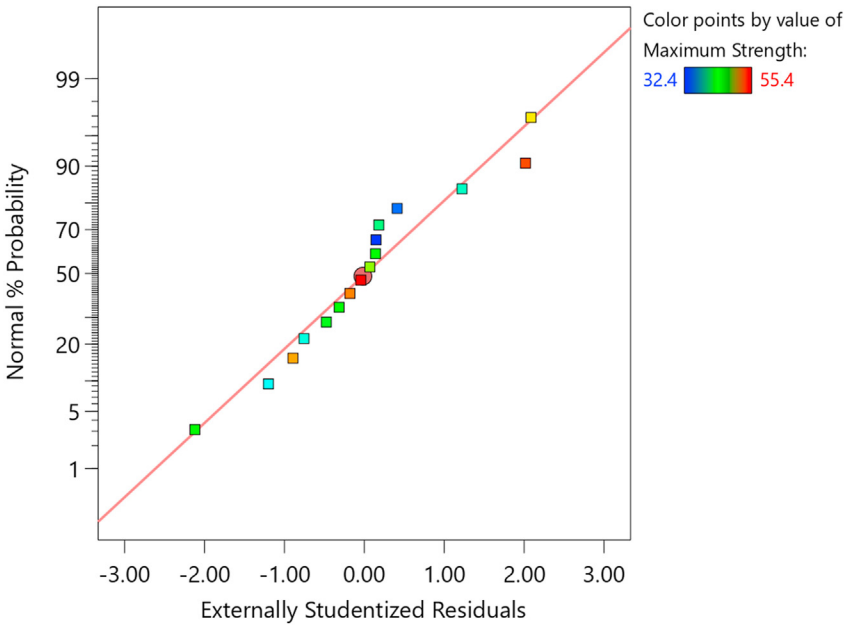


**Fig. 6.** Normal plot of residuals for maximum tensile strength.

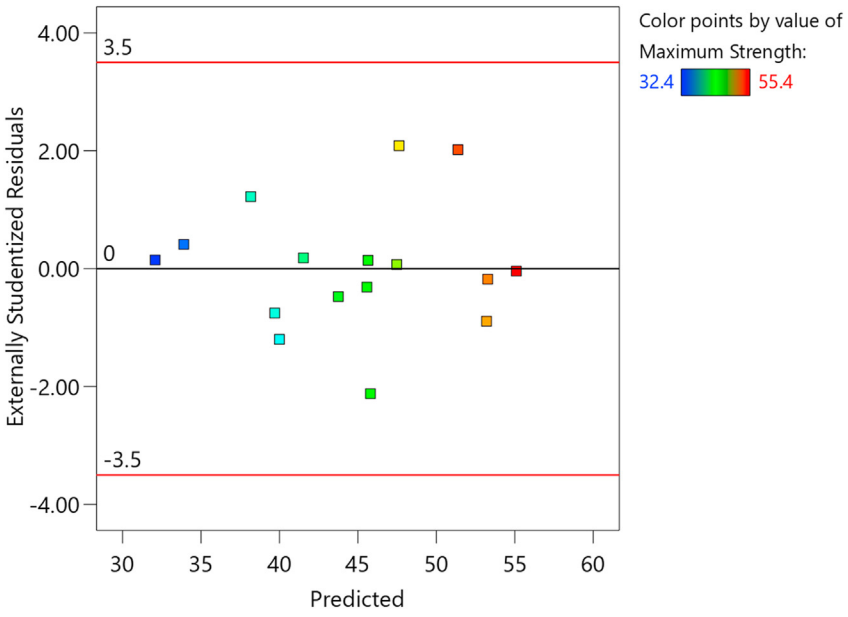


**Fig. 7.** A plot of residuals versus predicted for maximum tensile strength.

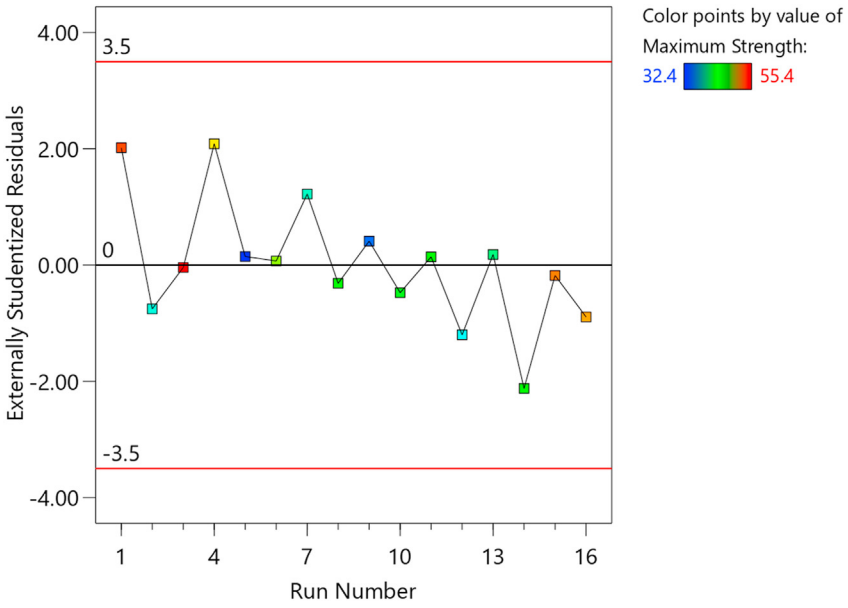


**Fig. 8.** Residuals versus run plot for maximum tensile strength.

Therefore, the factor levels for infill percentage would be 10 and 40%. Fig. 3 illustrates the infill patterns at 40% infill.

## 3. Results and analysis

Testing was carried out by a Zwick Roell zwickiLine z2.5 materials testing machine. The specimens were fitted into the tensile jaws, checked for alignment, and then pretensioned to eliminate compressive forces and improve repeatability of the results. The test speed was set to 5 mm/min. Following each test, the tensile test data were collected and recorded for analysis. In this section, results of tensile tests are presented first. Then, significant effects in the half-normal probability plot for both ultimate strength and print time are identified. In the last step, model assumptions before performing the DOE analysis are checked for each response separately.

The tensile test results achieved for sixteen samples, according to the design of experiment factors, are presented in Fig. 4. The process parameters of all samples (S1–S16) are displayed in Table 2.

Once the samples were tensile tested, the response data was collected in the randomized run order given by Design-Expert software. Table 2 illustrates the design runs with the responses.

### 3.1. Screening for maximum tensile strength

After collecting the randomized run order by Design-Expert software, the next step is to identify the significant effects in the half-normal probability plot. This is achieved by conducting a “Fat

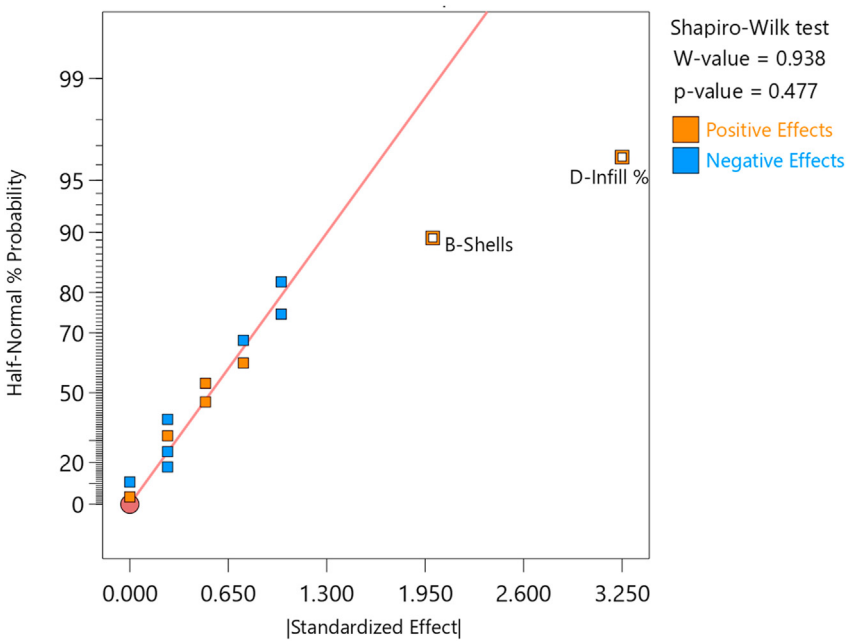


**Fig. 9.** Half-normal probability plot of subplot effects for print time.

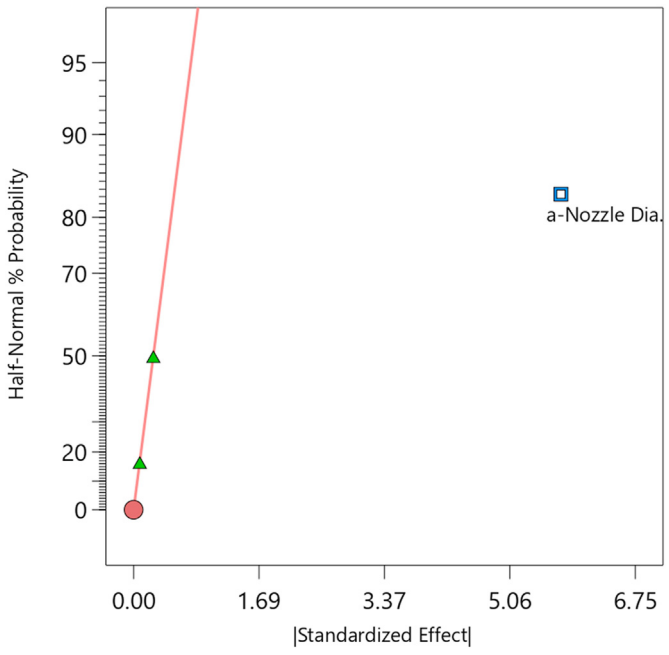


**Fig. 10.** Half-normal probability plot of whole-plot effects for print time.

Pencil" test [20]. A fat pencil test is an informal approach that's useful as a quick visual assessment. This assessment is conducted by lying a pencil on top of the fitted line. If it covers all the data points on the plot, the data are probably normal. If points are far enough from the fitted line that they are visible beyond the edges of the fat pencil, the data are considered significant. As useful as this test is, it is not a substitute for the statistical inference of the normality test itself. The effects that were found to be greater than the noise σ were the number of outer shells (B), infill percentage (D), the interaction of the number of outer shells and infill percentage (BD), and infill pattern (E). The plot of these effects is illustrated in Fig. 5.

Additionally, these effects were reviewed for significance using ANOVA tables. The ANOVA table can be seen in Table 3. Factors considered insignificant (P-value greater than 0.05) were removed from the model, as they have no effect on the response. Based on the F-values, the number of shells (B) appear to have the most significance, followed by nozzle diameter (a), infill percentage (D), and infill pattern (E).

### 3.2. Checking assumptions for maximum ultimate strength

It is critical to check model assumptions before performing the DOE analysis, because if assumptions are not met, then the conclusions from the analysis may not be valid. As such, prior to performing an interpretation of the model, the diagnostic plots were checked for any violation of assumptions. The assumptions that were implied for the data were the assumption of normal distribution and independent residuals with constant variance. The normal probability plot of residuals uses the fat pencil test to subjectively determine whether the error is normally distributed. Fig. 6 confirms that there is a normal distribution.

Fig. 7 shows a plot of residuals versus predicted for maximum tensile strength. This plot is used to check for constant variance, non-linearity, and outliers. Based on the data, it supports the notion of constant variance since there is no pattern observed.

Fig. 8 shows a plot of residuals versus run for maximum tensile strength. The purpose of this figure is to check for any form of non-independence of the error terms. As the name suggests, the result is a scatter plot with residuals on the y-axis and the order in which

**Table 4**
ANOVA table for print time, fixed effects [Type III], performed by REML (restricted maximum likelihood) analysis.

| Source | Term df | Error df | F-value | p-value | |
|---|---|---|---|---|---|
| **Whole-plot** | 1 | 12.00 | 102.39 | <0.0001 | Significant |
| a-Nozzle dia. | 1 | 12.00 | 102.39 | <0.0001 | |
| **Subplot** | 2 | 12.00 | 22.55 | <0.0001 | Significant |
| B-Shells | 1 | 12.00 | 12.39 | 0.0042 | |
| D-Infill % | 1 | 12.00 | 32.71 | <0.0001 | |

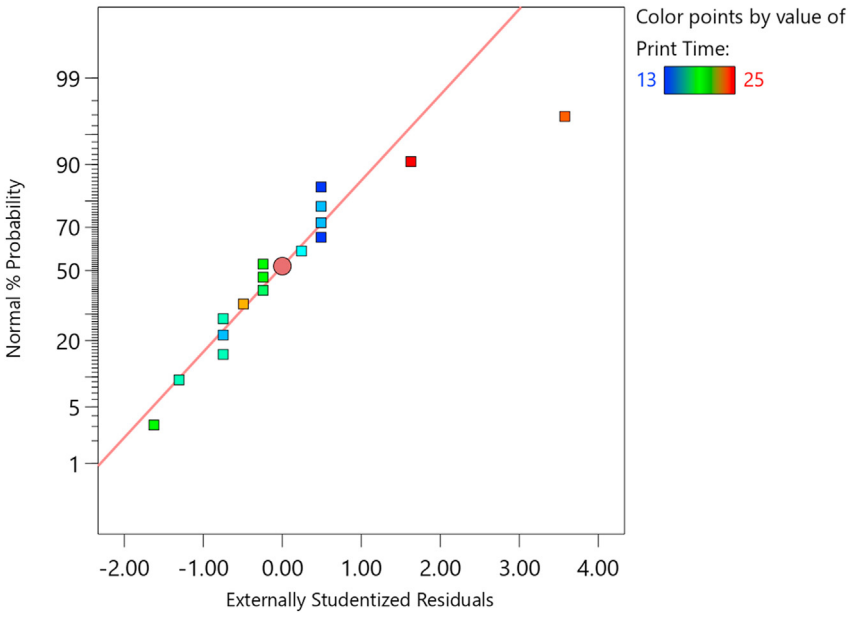


**Fig. 11.** Normal plot of residuals for print time.

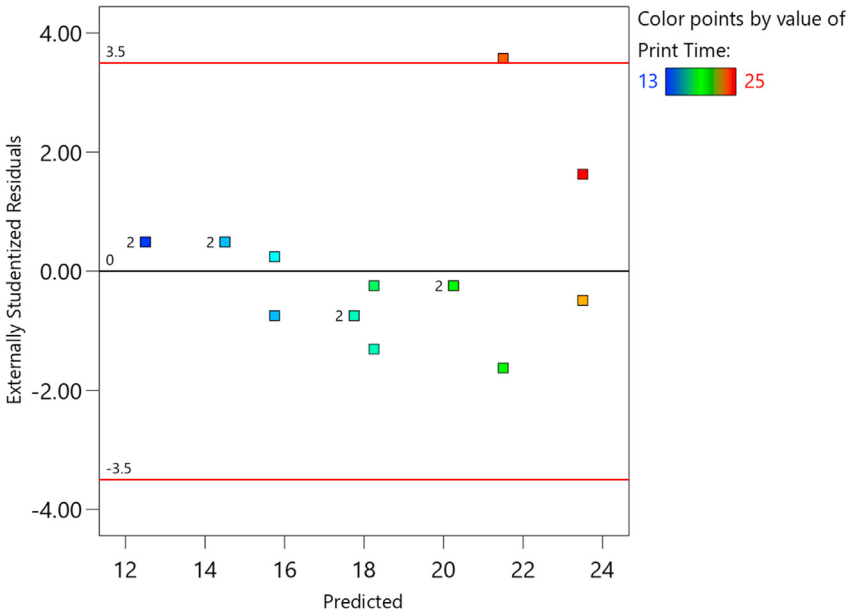


**Fig. 12.** A plot of residuals versus predicted for print time.

the data were collected (also referred to as the run) on the x-axis, i.e. the residuals should "bounce" randomly around the residual line [21]. However, the residuals versus run plot generated from the experiment do not illustrate independence due to the slight downward trend. This indicates that there exists a lurking variable within the experiment that was not accounted for. This revelation could be the topic of future research opportunities.

### 3.3. Screening for print time

The screening process was then repeated for the Print Time response. The effects were reviewed for significance using the ANOVA tables and the Half-Normal Probability Plot. Based on the "Fat Pencil" visual test, as seen in Figs. 9 and 10, and through reviewing the P and F-values in the ANOVA tables in Table 4, three significant factors were identified out of the original five. The nozzle diameter (a) appears to be the most significant, followed by the infill percentage (D), and the number of outer shells (B).

The ANOVA table for print time can be seen in Table 4. Factors considered insignificant (P-value greater than 0.05) were removed from the model. Based on the F-values, the infill percentage (D) appears to have the most significance, followed by the number of shells (B).

### 3.4. Checking assumptions for print time

Normality, constant variance, and linear independence are illustrated in Figs. 11–13. As shown, the normal probability plot of

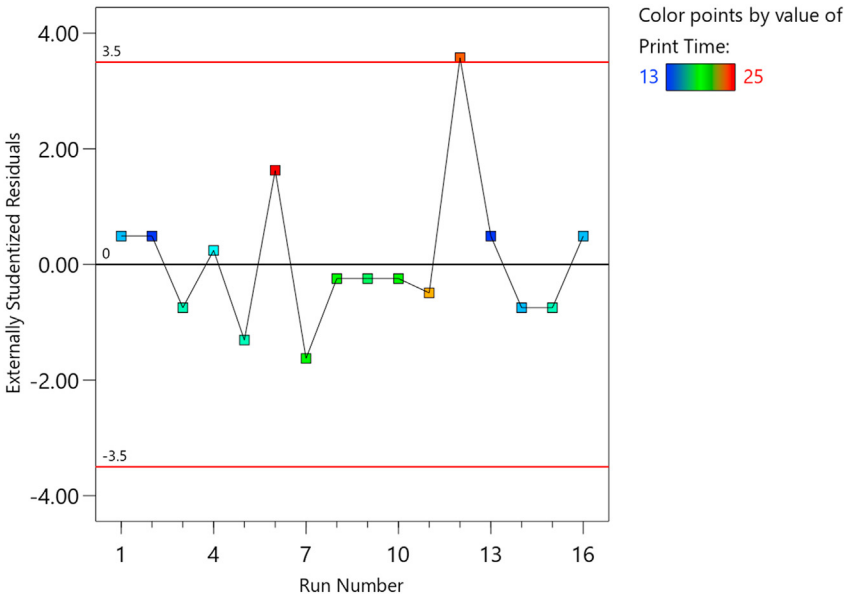


**Fig. 13.** A plot of residuals versus run for print time.

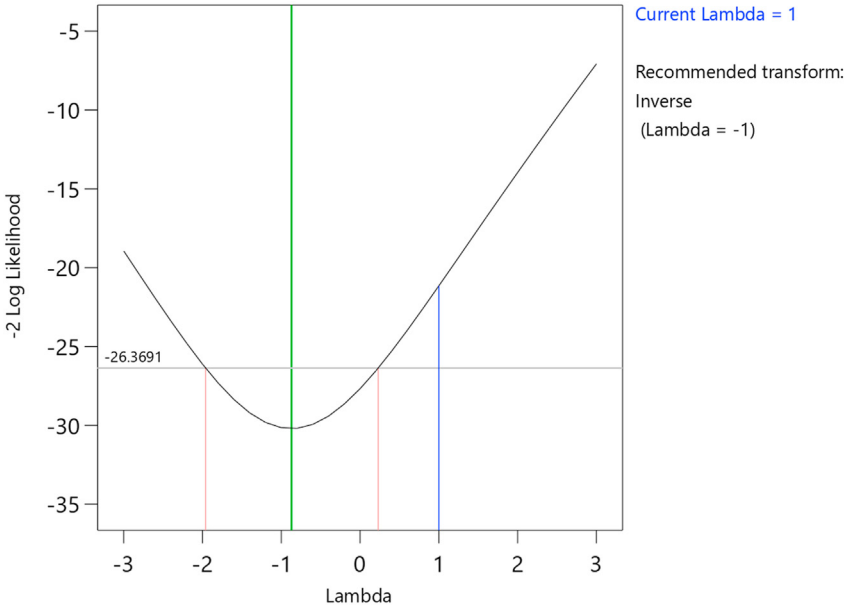


**Fig. 14.** Box–Cox plot for print time.

residuals failed the "Fat Pencil" test with one data point off the fitted line.

The results of residuals versus predicted and run for print time are shown in Figs. 12 and 13. As seen, there is one point outside the variance range when checking for constant variance. Six runs showed little variance when checking for independence, along with one point being outside the variance range. Hence, an inverse transformation on the response was then applied to account for the concerns found with the variance checks, which are discussed in the next section.

### 3.5. Screening/checking assumptions after transformation

Box–Cox plot provided in Fig. 14 recommends an inverse transform of print time. The transformed ANOVA table was reviewed for significance, as shown in Table 5. Normality was then verified with the "Fat Pencil" test in Fig. 15. Constance variance and linear independence were also verified in Figs. 16 and 17.

**Table 5**
Transformed (inverse) ANOVA table for print time, fixed effects [Type III], performed by REML (restricted maximum likelihood) analysis.

| Source | Term df | Error df | F-value | p-value | |
|---|---|---|---|---|---|
| **Whole-plot** | 1 | 12.00 | 207.69 | <0.0001 | Significant |
| a-Nozzle dia. | 1 | 12.00 | 207.69 | <0.0001 | |
| **Subplot** | 2 | 12.00 | 46.36 | <0.0001 | Significant |
| B-Shells | 1 | 12.00 | 29.66 | 0.0001 | |
| D-Infill % | 1 | 12.00 | 63.05 | <0.0001 | |

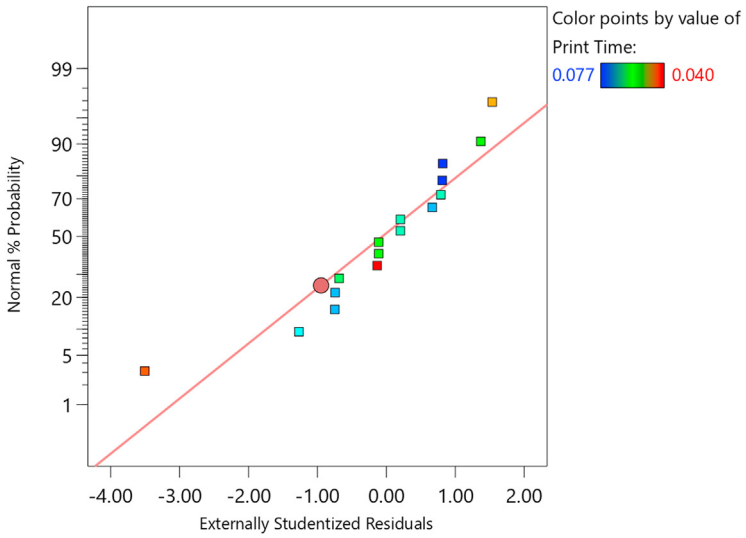


**Fig. 15.** Transformed normal plot of residuals for print time.

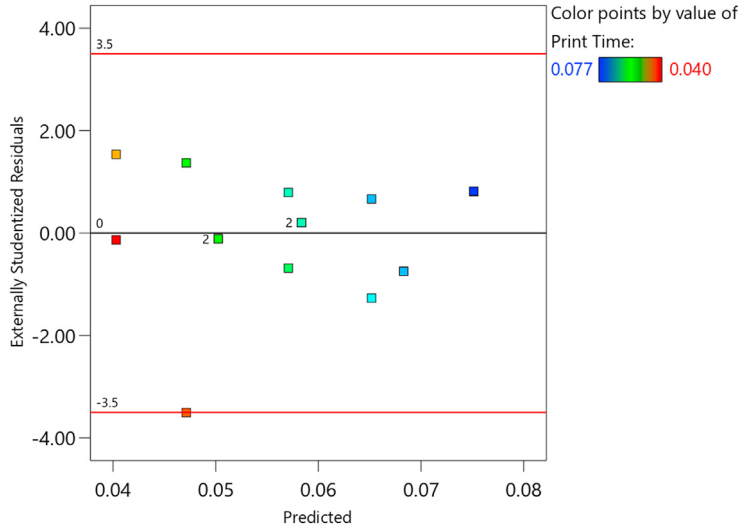


**Fig. 16.** Transformed residuals versus predicted plot for print time.

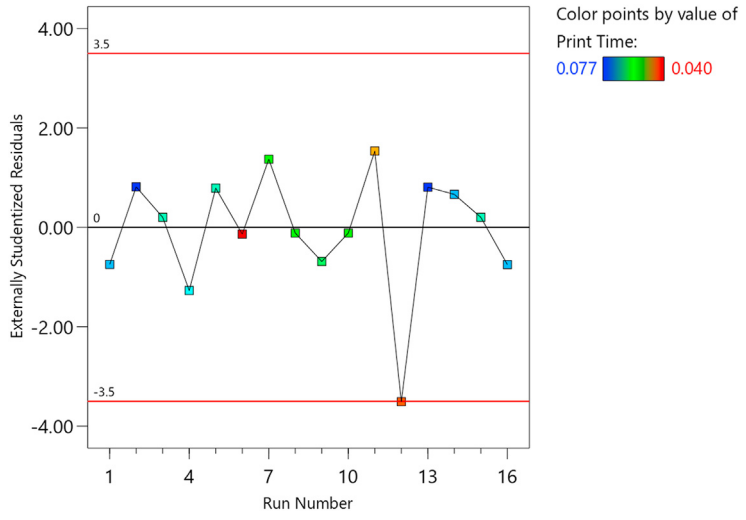


**Fig. 17.** Transformed residuals versus run plot for print time.

## 4. Interpolation

### 4.1. Maximum tensile strength

The results of tensile strength can be seen in Figs. 18 and 19. Based on the model, it appears that the number of outer shells (B) remains to be the dominant factor in the outer shells/infill percentage interaction (BD). Increasing the number of outer shells significantly improves the maximum tensile strength of which the test specimen can withstand. The infill percentage affects the maximum tensile strength at lower numbers of outer shells, although it does not significantly improve it at a higher number of outer shells. Additionally, the 0.6 mm nozzle improves the maximum tensile strength across all levels of infill percentages and number out shells.

### 4.2. Print time

The results of the print time study can be seen in Fig. 20. Of course, the data supports that lower infill percentages and a lower number of outer shells will reduce print time. Based on the model, however, it appears that the nozzle diameter (a) remains to be the most significant factor for improving print time.

### 4.3. Optimization recommendations

In this section, optimization was reviewed for minimizing print time while simultaneously maximizing the mechanical properties using the derived regression models. An optimum setting of the factors is summarized in Fig. 21. The recommendation is that the test specimen should be fabricated using a 0.6 mm nozzle, with four outer shells and 10% infill. If these process parameters are selected, less than 15 min is needed to print a part that can withstand a maximum strength of roughly 53.2 MPa.

Although temperature 215 °C is shown as a recommended parameter in Fig. 21, it was found printing at two selected temperatures (215 and 230 °C) does not influence the responses, while the nozzle diameters (0.4 and 0.6 mm) can influence the responses. The nozzle temperature results may contrast with results from previous studies [3,22]. This is because previous studies examined a broader temperature range, i.e. 205 and 260 °C [22]. Temperature effect on strength was examined more in detail in discussion section.

### 4.4. Confirmation

Lastly, confirmation points were run to validate that the model can predict actual outcomes. Two points within the ranges of the factors, but not those used to build the model, were selected as the confirmation points; one for the optimum settings for the 0.4 mm nozzle and the other for the optimum settings for the 0.6 mm nozzle. The details of these points are provided in Table 6. Three observations were run at each point. The print time and ultimate strength of each are presented in Table 7.

The averages of these runs were then compared to the predicted interval. The model was confirmed since the observations at the optimum were within the prediction interval with a confidence value of 95%. The results from Design Expert can be seen in Table 8.

## 5. Discussion

Based on the ANOVA model established in this study, the FDM process parameters have diverse effects on part strength

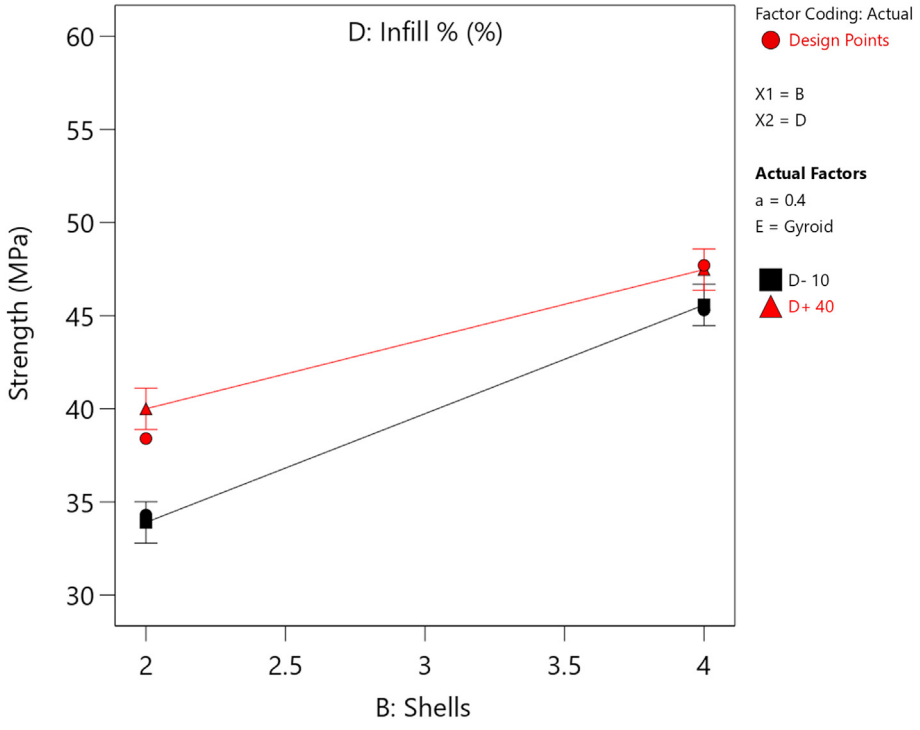


**Fig. 18.** Model graphs BD interaction (0.4 mm nozzle).

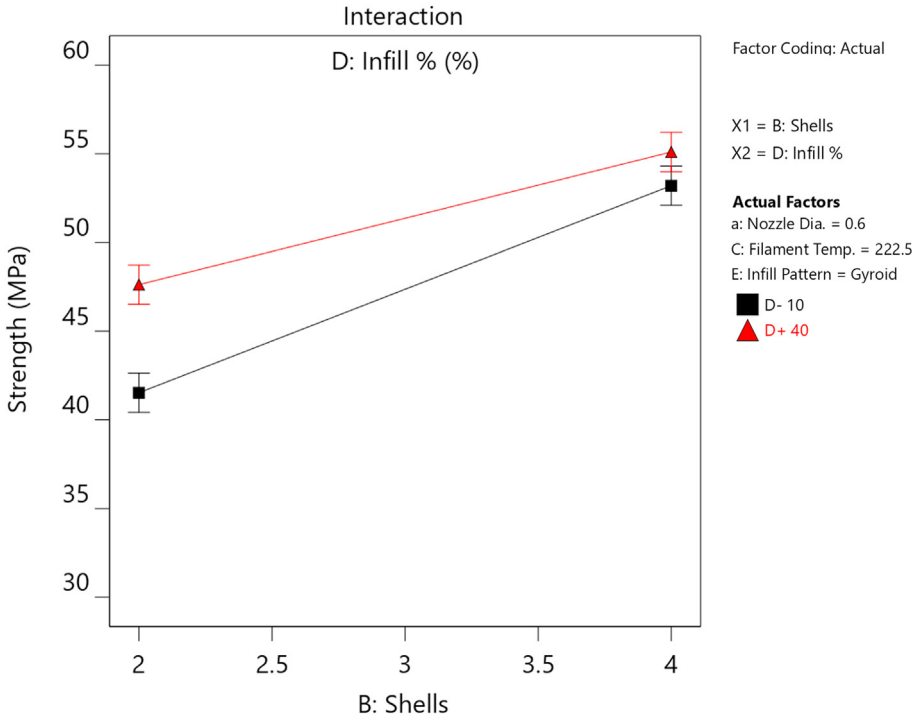


**Fig. 19.** Model graphs BD interaction (0.6 mm nozzle).

and print time. The selected process parameters, such as nozzle diameter, the number of outer shells, extrusion temperature, infill percentage, and infill pattern have influence on the print time and part strength to a certain extent. It is well known that the thermal conditions, such as previously deposited layer temperature and nozzle temperature (extrusion temperature), are crucial in determining the bonding quality between layers. This study also investigated the effect of various nozzle temperatures to show how much part strength is obtained when increasing temperature from 205 °C

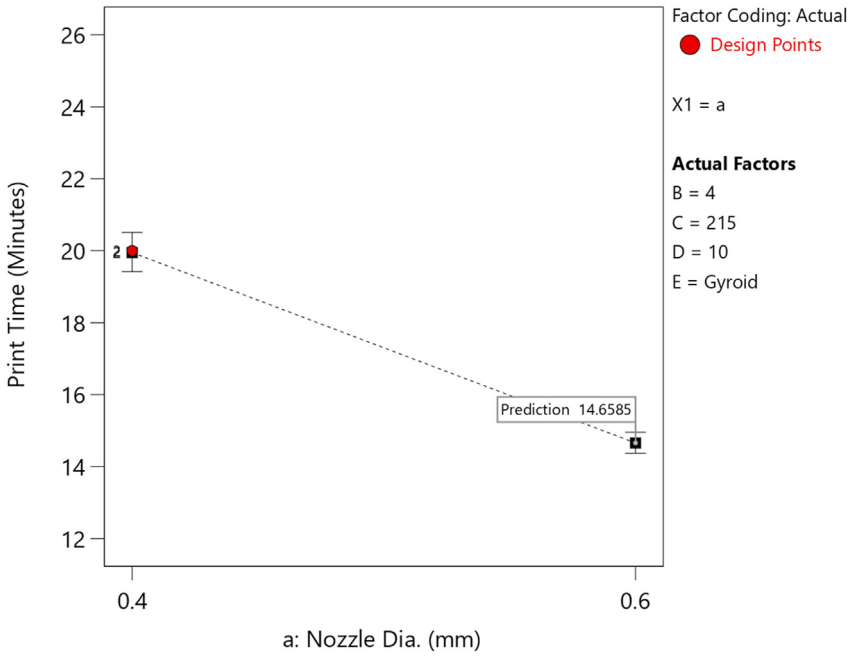


**Fig. 20.** Model graphs one factor.

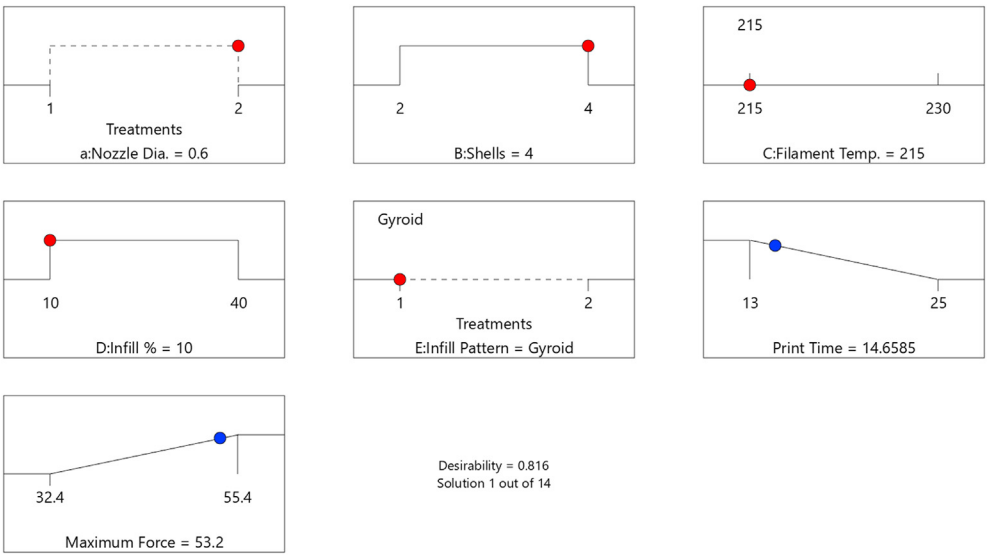


**Fig. 21.** Optimization recommendations.

**Table 6**
Process parameters of two confirmation points used to validate the model.

| Factor | Point 1 | Point 2 |
|---|---|---|
| Nozzle diameter | 0.4 | 0.6 |
| Number of outer shells | 4 | 4 |
| Extrusion temperature | 215 | 215 |
| Infill percentage | 10 | 10 |
| Infill pattern | Gyroid | Gyroid |

to 230 °C. Fig. 22 shows that higher nozzle temperatures resulted in higher part strength, mainly because of formation of less void. Based on printing temperature, three common voids are normally observed in the FDM parts, which are demonstrated in Fig. 23. If the nozzle temperature is low, the chance to increase the previously deposited layer and create a large bonding area is less since there is the lack of molecular diffusion of polymer chains, Fig. 23c. This leads to weak bonding between the layers. In this study, large voids are observed in lower temperature such as 205 °C, see Fig. 24. As the nozzle temperature increases, bonding area increases. This leads to a neck growth between adjacent filaments, see Figs. 23c and 24b. This causes the polymer chains to diffuse to one another and increase randomization of polymer chains across the filaments' interface, which subsequently provides stronger adhesion.

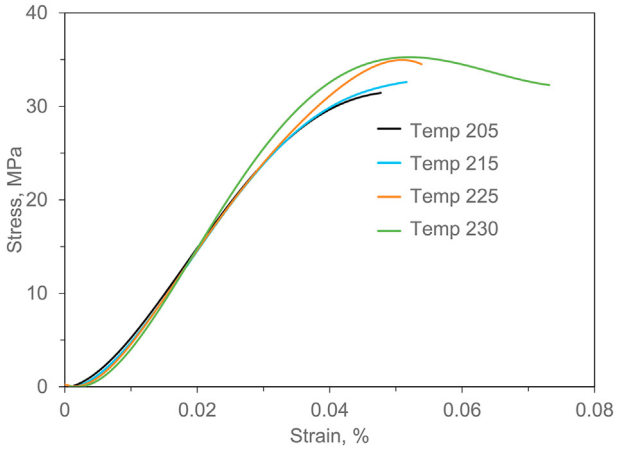


**Fig. 22.** Effect of four nozzle temperatures on strength of FDM parts.

**Table 7**
Print time and ultimate strength for three observations for two confirmation points.

| Confirmation point 1 | | Confirmation point 2 | |
|---|---|---|---|
| Print time (minutes) | Ultimate strength (MPa) | Print time (minutes) | Ultimate strength (MPa) |
| 20 | 42.27 | 15 | 51.26 |
| 20 | 43.95 | 15 | 51.05 |
| 20 | 42.92 | 15 | 50.52 |

**Table 8**
Comparison of experimental results with those obtained from the model establish design expert, two-sided, confidence = 95%.

| Response | Predicted mean | Total std dev | n | SE pred | Error df | 95% PI low | Data mean | 95% PI high |
|---|---|---|---|---|---|---|---|---|
| Print time | 20.25 | 1.13652 | 3 | 0.868028 | 12 | 18.3587 | 20 | 22.1413 |
| Strength | 45.575 | 1.71296 | 3 | 1.48801 | 4.68299 | 41.6707 | 43.0467 | 49.4793 |
| Print time | 14.5 | 1.13652 | 3 | 0.868028 | 12 | 12.6087 | 15 | 16.3913 |
| Strength | 53.2 | 1.71296 | 3 | 1.48801 | 4.68299 | 49.2957 | 50.9433 | 57.1043 |

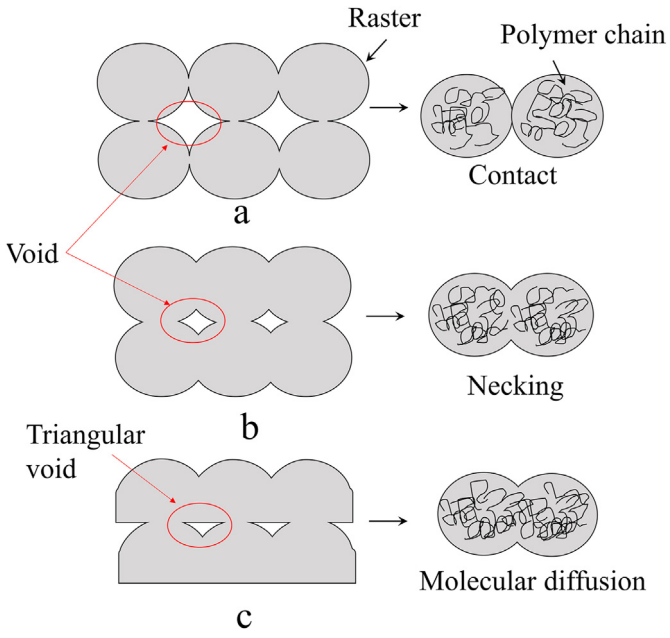


**Fig. 23.** Three common voids observed in the FDM parts.

Although nozzle temperature has a meaningful influence on the part strength, the number of outer shells, infill percentage, the interaction of those factors, nozzle diameter, and infill pattern were significant factors in increasing strength based on the ANOVA model. Increasing the number of outer shells significantly improves the ultimate strength of the test specimen. It was also demonstrated that a higher percentage of infill density, 40% compared with 10%, improves part strength by increasing the print time, which leads to increase overall fabrication cost. Therefore, a tradeoff among these factors should be determined if process efficiency is of interest.

According to the ANOVA model, the nozzle diameter appears to be the most significant factor to improving print time followed by the infill percentage and the number of outer shells. It is worth noting that the larger nozzle diameter improves the part strength significantly, as shown in Fig. 4 and Table 2. The main reason for the strength decreases in smaller nozzle diameter is attributed to larger surface to volume ratio. The beads extruded from smaller nozzle have larger surface to volume ratio compared with those extruded from larger nozzle. A thermoplastic with larger surface to volume ratio may exchange heat with the environment in a faster rate. If the thermoplastic loses its heat before diffusing to the previously deposited layer, it generates weak bonding between the layers. The lack of bonding between PLA layers are demonstrated in the SEM images, shown

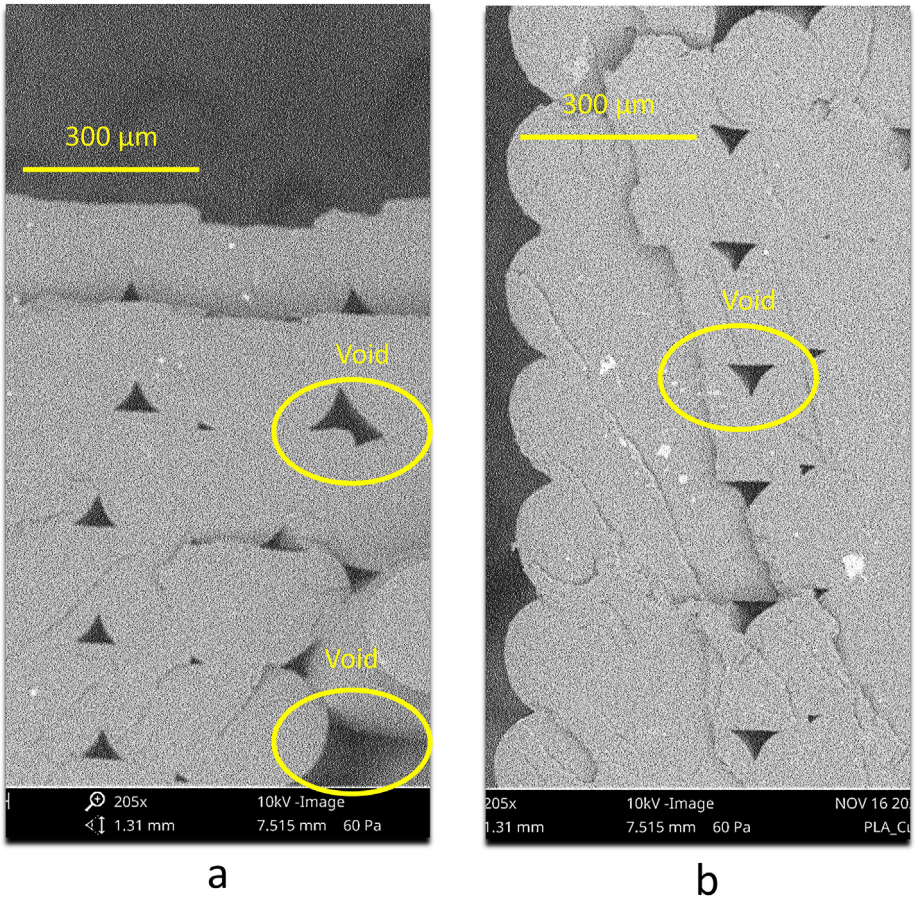


**Fig. 24.** SEM images revealing void in FDM parts printed with (a) 205 °C (b) 230 °C nozzle temperatures.

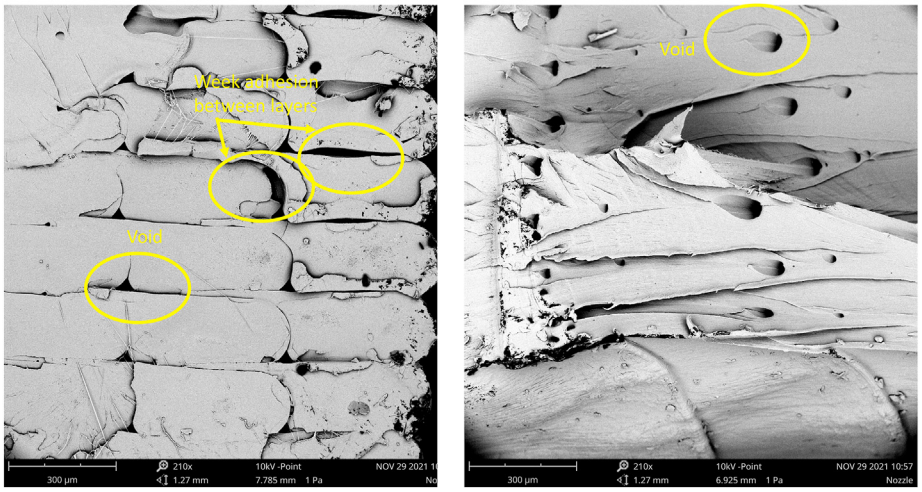


**Fig. 25.** SEM images revealing adhesion between layers in FDM parts printed with (a) 0.4 mm nozzle (b) 0.6 mm nozzle.

in Fig. 25a. Lack of molecular diffusion of polymer chains was signifyingly reduced in the parts extruded from 0.6 nozzle diameter, Fig. 25b.

## 6. Conclusion

In this study, design of experiments (DOE) was employed as a cost-effective tool for optimization and conducting the experiment. Analysis of variance (ANOVA) was employed to verify the model significance. The model was confirmed with two confirmation points with a confidence value of 95%. Then the model was used to assess the ultimate strength and print time of additively manufactured PLA with consideration to nozzle diameter, the number of outer shells, extrusion temperature, infill percentage, and infill pattern. The conclusions obtained in this study can be classified in two main sections. The first section is used to investigate the impact of process parameters on part strength and to elucidate which has the greatest impact on a part strength. The second section revealed how to reduce the print time without sacrificing significant strength. The latter was driven by the need to save operating cost since there is a growing demand to lightweight structures.

The data presented indicates that the number of outer shells, infill percentage, the interaction of those factors, nozzle diameter, and infill pattern were significant factors on the mechanical properties. Increasing the number of outer shells significantly improves the ultimate strength of the test specimen. The infill percentage affects the ultimate strength at lower numbers of outer shells, while it does not significantly improve the ultimate strength at a higher number of outer shells. Additionally, the 0.6 mm nozzle and gyroid infill pattern improves the ultimate strength across all levels of infill percentages and number out shells.

Furthermore, the nozzle diameter, infill percentage, and the number of outer shells were significant factors in reducing print time. The nozzle diameter was the most significant factor for improving print time. Using a 0.6 mm nozzle will improve print time across all infill percentages and the number of outer shells. Of course, the data also supports that lower infill percentages and a lower number of outer shells reduce print time. Based on the model created in this research, it is recommended that using a larger nozzle diameter (0.6 mm nozzle) with more outer shell (four shells) and 10% infill can minimize print time without sacrificing significant strength compared with a part fabricated with 40% infill.

## Conflicts of interest

The authors declare that there is no conflicts of interest.

## References

[1] G.J. Johnson, Encyclopedia of Analytical Science, second ed., 2005.
[2] E.A. Campo, Selection of Polymeric Materials How to Select Design Properties from Different Standards Plastics Design, Library, 2008.
[3] V.E. Kuznetsov, A.N. Solonin, A.G. Tavitov, O.D. Urzhumtsev, A.H. Vakulik, Increasing of Strength of FDM (FFF) 3D Printed Parts by Influencing on Temperature-Related Parameters of the Process, 2018, pp. 1–32, https://doi.org/10.20944/preprints201803.0102.v2.
[4] R. Srinivasan, P. Prathap, A. Raj, S.A. Kannan, V. Deepak, Influence of fused deposition modeling process parameters on the mechanical properties of PETG parts, Mater. Today Proc. 27 (2020) 1877–1883, https://doi.org/10.1016/j.matpr.2020.03.809.
[5] N.P. Levenhagen, M.D. Dadmun, Improving interlayer adhesion in 3D printing with surface segregating additives: improving the isotropy of acrylonitrile–butadiene–styrene parts, ACS Appl. Polym. Mater. 1 (2019) 876–884, https://doi.org/10.1021/acsapm.9b00051.
[6] J.M. Chacón, M.A. Caminero, E. García-Plaza, P.J. Núñez, Additive manufacturing of PLA structures using fused deposition modelling: effect of process parameters on mechanical properties and their optimal selection, Mater. Des. 124 (2017) 143–157, https://doi.org/10.1016/j.matdes.2017.03.065.
[7] S. Ziemian, M. Okwara, C.W. Ziemian, Tensile and fatigue behavior of layered acrylonitrile butadiene styrene, Rapid Prototyp. J. 21 (2015) 270–278, https://doi.org/10.1108/RPJ-09-2013-0086.
[8] C.S. Lee, S.G. Kim, H.J. Kim, S.H. Ahn, Measurement of anisotropic compressive strength of rapid prototyping parts, J. Mater. Process. Technol. 187–188 (2007) 627–630, https://doi.org/10.1016/j.jmatprotec.2006.11.095.
[9] D. Corapi, G. Morettini, G. Pascoletti, C. Zitelli, Characterization of a polylactic acid (PLA) produced by fused deposition modeling (FDM) technology, Procedia Struct. Integr. 24 (2019) 289–295, https://doi.org/10.1016/j.prostr.2020.02.026.
[10] B. Redwood, F. Schoffer, B. Garret, The 3D printing handbook: technologies, Des. Appl. D 3 (2017).
[11] G.A. Johnson, J.J. French, Evaluation of infill effect on mechanical properties of consumer 3D printing materials. https://ojs.imeti.org/index.php/AITI/article/view/1010, 2018.
[12] K.L. Alvarez C, R.F. Lagos C, M. Aizpun, Investigating the influence of infill percentage on the mechanical properties of fused deposition modelled ABS parts, Ing. Investig. 36 (2016) 110–116, https://doi.org/10.15446/ing.investig.v36n3.56610.
[13] K. Abouzaid, S. Guessasma, S. Belhabib, D. Bassir, A. Chouaf, Thermal mechanical characterization of copolyester for additive manufacturing using

FDM, Int. J. Simul. Multidiscip. Des. Optim. 10 (2019) A9, https://doi.org/10.1051/smdo/2019011.
[14] V.D. Sagias, K.I. Giannakopoulos, C. Stergiou, Mechanical properties of 3D printed polymer specimens, Procedia Struct. Integr. 10 (2018) 85–90, https://doi.org/10.1016/j.prostr.2018.09.013.
[15] C. Vălean, L. Marşavina, M. Mărghitaşl, E. Linul, J. Razavi, F. Berto, Effect of manufacturing parameters on tensile properties of FDM printed specimens, Procedia Struct. Integr. 26 (2020) 313–320, https://doi.org/10.1016/j.prostr.2020.06.040.
[16] Prusa i3 MK3S, (n.d.). https://www.prusa3d.com/product/original-prusa-mini-3/.
[17] ASTM-D638-14, Standard Test Method for Tensile Properties of Plastics, ASTM Stand, 2014, pp. 1–15.
[18] PrusaSlicer, (n.d.). https://www.prusa3d.com/prusaslicer/.
[19] E3D, (n.d.). https://e3d-online.com/.
[20] D.C. Montgomery, Design and Analysis of Experiments, John Wiley & Sons, 2017.
[21] Applied Regression Analysis, (n.d.).
[22] M. Foppiano, A. Saluja, K. Fayazbakhsh, The effect of variable nozzle temperature and cross-sectional pattern on interlayer tensile strength of 3D printed ABS specimens, Exp. Mech. 61 (2021) 1473–1487, https://doi.org/10.1007/s11340-021-00757-y.